



**HAL**  
open science

## Bottom-up solution chemistry approaches for nanostructured thermoelectric materials

Roland Benoit, Virginie Hornebecq, François Weill, Lollita Lecren, Xavier Bourrat, Mona Tréguer-Delapierre

### ► To cite this version:

Roland Benoit, Virginie Hornebecq, François Weill, Lollita Lecren, Xavier Bourrat, et al.. Bottom-up solution chemistry approaches for nanostructured thermoelectric materials. *Journal of Materials Chemistry A*, 2013, 1 (45), pp.14221-14226. 10.1039/C3TA12896B . hal-00880782

**HAL Id: hal-00880782**

**<https://hal.science/hal-00880782>**

Submitted on 30 Jun 2022

**HAL** is a multi-disciplinary open access archive for the deposit and dissemination of scientific research documents, whether they are published or not. The documents may come from teaching and research institutions in France or abroad, or from public or private research centers.

L'archive ouverte pluridisciplinaire **HAL**, est destinée au dépôt et à la diffusion de documents scientifiques de niveau recherche, publiés ou non, émanant des établissements d'enseignement et de recherche français ou étrangers, des laboratoires publics ou privés.

## Bottom-up solution chemistry approaches for nanostructured thermoelectric materials

Roland Benoit,<sup>\*a</sup> Virginie Hornebecq,<sup>b</sup> François Weill,<sup>c</sup> Lollita Lecren,<sup>d</sup> Xavier Bourrat<sup>e</sup> and Mona Tréguer-Delapierre<sup>c</sup>

Despite recent progress in the development of the thermoelectric power factor, improvement in the efficiency of thermoelectric materials remains limited. Over the past decade, almost all the significant advances have been made by the development of nanostructured materials. Both theoretical studies and experimental results bring out three main avenues of research for optimizing the engineering of these materials: (i) quantum confinement, (ii) phonon-blocking/electron transmitting and (iii) electron filtering barrier structures. The optimization of one or several of these parameters is dependent on the design of the materials that are very complex to synthesize and, for this reason, many of the studies remain merely of theoretical interest. A material allowing the optimization of all of these parameters is thus proposed. It is based on a nanostructured material (starting from a mesoporous matrix), within which it is possible to control the size and spacing of nanoparticles. In addition, some confined bismuth nanoparticles in this type of structure transform to a cubic phase, making it possible to avoid orientation problems related to the effective masses.

DOI: 10.1039/XXXXXXXXXX

### Introduction

Despite efforts to enhance the thermoelectric figure of merit ( $ZT$ ) over the past forty years, it has been proved that it is not possible to experimentally exceed a  $ZT$  value of 3, which is the necessary threshold to attain competitive energy conversion compared to conventional mechanical systems. The  $ZT$  is defined as  $ZT = S^2\sigma T/(k_L + k_e)$  where  $S$  is the Seebeck coefficient,  $\sigma$  is the electrical conductivity,  $T$  is the absolute temperature,  $k_L$  is the lattice thermal conductivity and  $k_e$  is the carrier thermal conductivity. Nevertheless, many theoretical studies show that it is possible to reach  $ZT$  values higher than this limit<sup>1,2</sup> and one of the most promising routes is the use of nanostructured materials.<sup>3</sup> Indeed, these materials offer the opportunity to tailor physical properties such as electricity and heat transport that are associated with an electron-filtering effect and phonon confinement on the lattice.<sup>4,5</sup> Dresselhaus' group was one of the

first to show that 1D and 2D structures would be likely to reach a  $ZT$  value higher than 6.<sup>6,7</sup> Thermoelectric materials are currently studied and synthesized in various forms such as thin films,<sup>8,9</sup> nanotubes,<sup>10–12</sup> and, more recently, nanostructured materials.<sup>13–15</sup> These studies are generally carried out in the light of three criteria.

The first approach, widely applied in syntheses, consists of reducing the size of materials on a nanometric scale so as to generate quantum confinement.<sup>16</sup> The objective is to adjust the physical properties such as the mean free path of the electrons, the effective mass of the electrons and the holes, as well as the thermal and electronic conductivities or even the density of state at the Fermi level. Bismuth or bismuth compounds are one of the most intensively studied compounds because of the changes in their properties as a function of nanoparticle size.<sup>17</sup> In addition to the semi-metal–semiconductor transition extensively described in the literature,<sup>18,19</sup> this element has one of the largest mean-free paths ( $\sim 0.4$  nm at 4 K) and one of the smallest effective masses ( $\sim 0.001m_0$ ).<sup>20,21</sup> Recent studies on the effects of dimensionality show that the exploitation of thermoelectric properties would be optimal for particle sizes smaller than 20 nm.<sup>22,23</sup>

The second approach, based on phonon-blocking/electron-transmitting structures, consists of reducing thermal conductivity while maintaining electrical conductivity. The propagation of phonons can be limited by using materials with weak lattice thermal conductivity and/or by interfaces contained within the material.<sup>24</sup> This principle has led to the development of (i) QWRs (quantum wires), (ii) MQW (multiple

<sup>a</sup>CRMD UMR6619, Université d'Orléans, CNRS, 1B rue de la Férollerie, 45071 Orléans Cedex 2, France. E-mail: r.benoit@cnrs-orleans.fr; Fax: +33 238255377; Tel: +33 238255376

<sup>b</sup>Aix-Marseille Université, CNRS, MADIREL MATériaux Divisés, Interface, Réactivité, Electrochimie UMR 7246, 13397, Marseille, France. E-mail: Virginie.Hornebecq@univ-amu.fr; Fax: +33 4551850; Tel: +33 4551823

<sup>c</sup>CNRS, Université de Bordeaux, ICMCB, 87 Av. du Dr A.Schweitzer, Pessac, 33608, France. E-mail: treguer@icmcb-bordeaux.cnrs.fr; Fax: +33 540002761; Tel: +33 540006333

<sup>d</sup>Centre de Recherche Paul Pascal, CNRS-UPR 8641, 115 Avenue du Dr Schweitzer, F-33600 Pessac, France

<sup>e</sup>BRGM, 3 avenue C. Guillemin, BP36009, 45060 Orléans Cedex 2, France. E-mail: X.Bourrat@brgm.fr

quantum walls) and (iii) QDSL (quantum dot superlattices), that make possible the reconciling of these two parameters.<sup>25-27</sup>

Among these three types of materials QDSLs are those that allow obtaining high values of  $ZT$ s.<sup>28-30</sup> The recent studies of Yadav *et al.* carried out on quantum dot chains show that the thermoelectric power factor can be increased by a factor of 3.<sup>31</sup>

Lastly, the third criterion consists of filtering electrons according to their energy in order to differentiate hot electrons from cold electrons. In particular, this differentiation can be performed owing to the presence of barriers of potential within the structure. In this way, a discriminatory filtering with respect to the cold electrons, while at the same time maintaining electrical conductivity was observed.<sup>32,33</sup> This process leads to an enhancement of the Seebeck coefficient by a factor of 2 to 3.<sup>34</sup>

Among these various structures of thermoelectric materials, QDSLs offer the best prospects for improving the figure of merit. Recent studies have shown that using the thermionic<sup>35</sup> effect or tunnel<sup>36</sup> effect inside these nanostructured materials could lead to advances. However, it remains a challenging task to synthesize such materials, while, at the same time, optimizing these three criteria to improve the figure of merit  $ZT$ .

By taking the above studies into account, and especially the dimensional constraints, we propose new bottom-up solution chemistry approaches allowing the tailoring of physical properties described above. The goal is to be able to control: (i) the size of the nanoparticles, so as to adjust the effective mass of the electrons, (ii) the dimension of the interfaces in the material, to study the propagation of phonons and electrons, and (iii) the composition of these interfaces, to study the filtering of the electrons according to their energy. In this model, the size and spacing between the nanoparticles, that is, the density of the network can be adjusted by the conditions of synthesis. Fig. 1 shows some examples of the adjustment of materials.

A very simple method of synthesis involving a single step, and allowing the formation of these networks within a mesoporous matrix was therefore developed. In contrast to the classical physical or chemical synthesis methods that are mostly expensive and/or complex (deposition under ultra-high vacuum, many stages of chemical synthesis, problems of stability of the samples in air, *etc.*), we propose a versatile approach in which nanoparticles are *in situ* synthesized within the mesoporous matrix, by impregnation of a salt followed by its reduction using ionizing radiation. Hexagonally ordered mesoporous silica was selected for its variable pore size ranging from 1.5 to 10 nm, which is suitable for studying quantum

confinement as well as for its properties of weak thermal and electrical conductivity.<sup>37</sup> Bismuth metal was chosen as the nanoparticle constituent due to its high power-factor ( $S^2\sigma$ ) and its singular physical properties that are widely described in the literature.<sup>38</sup>

## Experimental

### (a) Synthesis procedure

A solution of precursor (bismuth perchlorate in 18 M $\Omega$  deionized water at a concentration of 0.06 mol L<sup>-1</sup>) and a solution of oxidizing radical interceptor agent (7 mol L<sup>-1</sup> isopropanol) were prepared. Ordered mesoporous silica was synthesized according to the procedure described in the literature.<sup>39,40</sup> All the chemicals used (BiOClO<sub>4</sub><sup>2-</sup>, propanol, TEOS) were of the highest purity commercially available from Aldrich or Acros. Fig. 2 shows the silica obtained after synthesis and before impregnation.

Mesoporous silica was initially placed at ambient temperature in a secondary vacuum of 10<sup>-6</sup> Pa to remove physisorbed species from the surface. Then, it was impregnated for 1 h, under partial vacuum at saturation vapour pressure, with the precursor solution containing isopropanol. The liquid-gas equilibrium was maintained by carrying out primary pumping on the impregnation mixture. Impregnated silica was then placed under an anaerobic atmosphere at 10<sup>-5</sup> Pa, introduced into a sealed glass cell, and then irradiated with gamma rays for one hour at 2 kGy.h<sup>-1</sup>. Growth of the nanoparticles is achieved by homogeneous reduction of the bismuth salt using ionizing radiation. The size and spacing between these nanoparticles are adjusted by the pore size of the mesoporous matrix, the radiation dose rate and the initial salt concentration. The growth of the nanoparticles is related to the gamma radiation dose as well as the dose rate. This growth is homogeneous within the mesoporous matrix for the whole of the nanoparticles. When the nanoparticles attain the size of the mesopores, atomic diffusion ceases. Bismuth ions begin to be depleted, which halts the growth of the nanoparticles in spite of the irradiation. After irradiation, the liquid containing the species that did not react is withdrawn and the mesoporous silica containing the nanoparticles is dried under primary vacuum while avoiding any contact with the atmosphere. The principle of this synthesis is illustrated in Fig. 3.

After drying, the silica containing the bismuth nanoparticles is less sensitive to oxidation. Furthermore, the nanoparticle

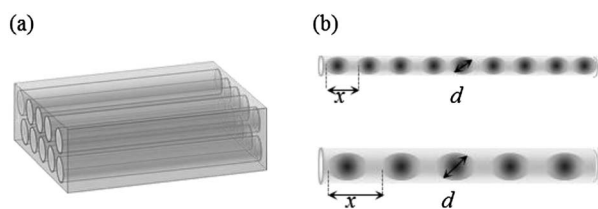


**Fig. 1** Illustration of possible adjustments of nanoparticles within a mesoporous matrix (a) using the suggested model (b) of the spacing  $x$  between nanoparticles and of the size of nanoparticles  $d$ .

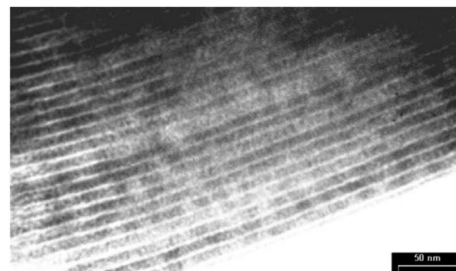


**Fig. 2** TEM micrograph of mesoporous silica with an internal channel diameter of 7 nm.

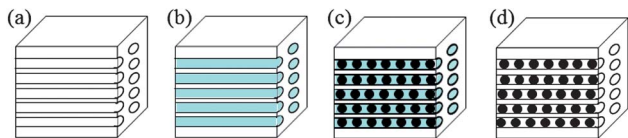


**Fig. 3** Schematic diagram of *in situ* nanoparticle synthesis within ordered mesoporous silica, (a) initial state; (b) impregnated bismuth salt; (c) after gamma irradiation, with bismuth nanoparticles and a liquid phase; (d) after drying under vacuum, with bismuth nanoparticles.

diameter being equal to the pore diameter of the mesoporous silica, gas diffusion remains limited. As a consequence, in a dry environment, the material does not show alteration by oxidation reactions during weeks. However, it is better to store it under inert gas conditions.

### (b) Characterization of materials

Powder X-ray diffraction measurements were recorded at room temperature on a Philips PW1820 diffractometer using Bragg–Brentano geometry with  $\text{CuK}\alpha$  radiation (50 mA, 40 kV). The investigated  $2\theta$  range was  $22\text{--}65^\circ$ , in  $0.02^\circ$  steps, with 10 s counting time. Powder was fixed on a plastic piece in order to avoid any oxidation reaction during the data acquisition. Transmission electron microscopy (TEM) measurements were performed with a Philips CM30ST microscope, having a resolution of 0.2 nm. Small mesoporous silica fragments were placed on a copper grid covered with an amorphous holey carbon. The grid was then transferred to an electron microscope.

## Results and discussion

### (a) Controlling the size and spacing of incorporated Bi nanoparticles

Two hexagonally ordered mesoporous silica presenting a porous channel diameter of 4 and 7 nm were used as host matrices for the incorporation of Bi nanoparticles. Apart from the process of impregnation, the chemical composition of the silica surface is a key parameter in determining the quality of the final material, in terms of density and spacing of nanoparticles. The surface of the silica pores must be covered by silanol groups, implying a thermal treatment of silica at temperatures lower than  $450^\circ\text{C}$ . Fig. 4 compares the results

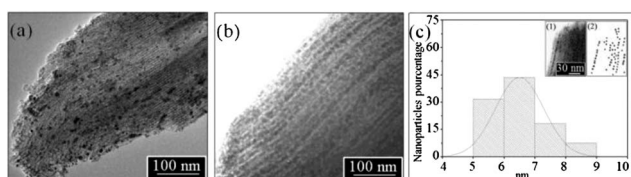


**Fig. 4** TEM micrograph of Bi NPs incorporated in ordered mesoporous silica (pore diameter = 7 nm) prepared after annealing treatment at (a)  $600^\circ\text{C}$ ; (b)  $400^\circ\text{C}$ . (c) Size distribution of bismuth metal nanoparticles in mesoporous silica (dpore = 7 nm), calculated from the TEM image (inset C.1) and analysis of images shown in inset C.2.

obtained on silica substrates with a mean pore diameter of 7 nm, treated at 400 and  $600^\circ\text{C}$ . In the latter case, the heat treatment reduces the concentration of silanols on the surface of the mesopores leading to a considerable decrease of the impregnation effectiveness (4a). Nanoparticle agglomerates related to an uncontrolled diffusion of the bismuth salt are observed, sometimes leading to the apparition of nanoparticles outside the mesoporous silica, and growing in the form of nanowires, or leading to the destruction of mesoporous silica during the growth of the nanoparticles. In contrast, a strong density of nanoparticles in the mesoporous channels of the silica matrix is evidenced when the mesoporous silica matrix is thermally treated at  $400^\circ\text{C}$ . The distribution and the size of these nanoparticles are uniform within the whole matrix. This material placed under argon remains stable for several months. In a previous study, we showed that, the bismuth nanoparticles rapidly oxidize in solution under ambient atmosphere and then disappear.<sup>41</sup>

We used image processing to calculate the nanoparticle size distribution starting from TEM images acquired for the compound obtained from the mesoporous silica matrix thermally treated at  $400^\circ\text{C}$ . These results that are based on the most contrasted nanoparticles compared to silica yield a particle size distribution centred at 7 nm with a low standard deviation (Fig. 4C, inset C.1 and C.2).

Observations of the material under high-magnification TEM confirm these values and show that nanoparticles have a mean diameter centred at 7 nm and a mean regular spacing of 2 nm. The modelling of the periodicity in the compound makes it possible to estimate a filling factor close to 80% at intervals of  $a = 9$  nm. The compositional analysis of this compound by EDX yields a Bi/Si ratio equal to 0.66, in agreement with the geometry of silica (wall thickness = 6 nm, diameter of channels = 7 nm) and its filling factor (Fig. 5). Furthermore, no chlorine trace was detected (within an EDS detection limit of 0.1 weight%).

The parameters defining the size and spacing of nanoparticles can be modified to meet the requirements for studying quantum confinement or thermoelectric properties.

With this in mind, we varied the size of the silica mesopores, the initial salt concentration and the radiation dose rate. A host silica matrix with 4 nm sized mesopores was used in this way. It corresponds to a reduction of almost 67% in the available internal volume compared to a silica matrix with 7 nm sized mesopores. Other operating conditions (salt concentration and

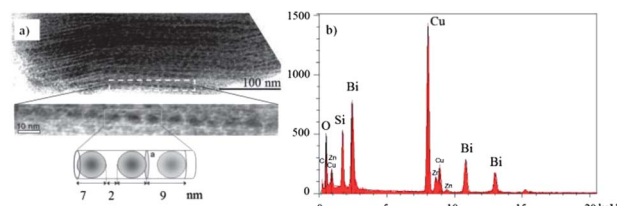


**Fig. 5** (a) Upper part: micrograph on various scales of bismuth metal nanoparticles developed *in situ* in a mesoporous silica (diameter pore = 7 nm); lower part: modelling of alignment of the nanoparticles (periodicity  $a = 9$  nm) used for calculating an impregnation ratio of 80%; (b) EDX spectrum of the compound deposited on a copper TEM grid (a): Bi = 40 at.%, Si = 60 at.%.

irradiation) were kept constant. Fig. 6 shows high-resolution TEM observations that evidence a silica matrix containing an alignment of nanoparticles with a diameter of 4 nm and a spacing of 4 nm maintained over a distance of several hundreds of nanometres. Decreasing the initial salt concentration by 50%, but maintaining the same conditions of irradiation gave the same result.

This experiment confirms that ions begin to be depleted within the silica when the size of the nanoparticles becomes equal to the diameter of the mesopores. Under these conditions, the *in situ* growth of the nanoparticles becomes negligible. The reduction of salt thus takes place essentially outside the mesoporous silica. This phenomenon allows us great flexibility in varying the initial salt concentration and the duration of irradiation.

Furthermore, when a mesoporous silica matrix with 4 nm pore size is used, the nanoparticle shape is less regular than the shape found in the first synthesis. This result can be explained by the fact that, at dimensions smaller than 4 nm, bismuth appears to be amorphous.<sup>42,43</sup> Moreover, at this scale, it was evidenced, for very short observation times, that the electron beam can modify the compound by spontaneously breaking up or displacing the nanoparticles. In particular, this phenomenon can probably explain the irregularities as shown in the example of Fig. 6: the position of the arrowed nanoparticle disturbs the periodic arrangement.

When the dose rate is decreased by 50%, while maintaining a constant dose, the radiolytic yield for the formation of Bi<sup>0</sup> decreases. The growth and the stabilization of the nanoparticles, which depend on the size, are limited. The nanoparticles are distributed heterogeneously within the mesoporous silica and have a mean diameter smaller than the mesopores. In this case, the diffusion of the bismuth salt is uncontrolled and the network of nanoparticles is disordered. The final compound is unstable with time. A 50% increase in the dose rate leads to an increase in the coalescence sites as well as in the final number of nanoparticles; the spacing between the nanoparticles, as for it, decreases.

In regard to the spacing between these nanoparticles, the proposed model depends on the thermionic emission between nanoparticles separated by distance  $x$ . Nanoparticles separated by 7 and 2 nm were *in situ* generated inside silica. This last value is in conformity with the optimization of thermoelectric properties in a QDSL described in the literature.<sup>29</sup> In view of our

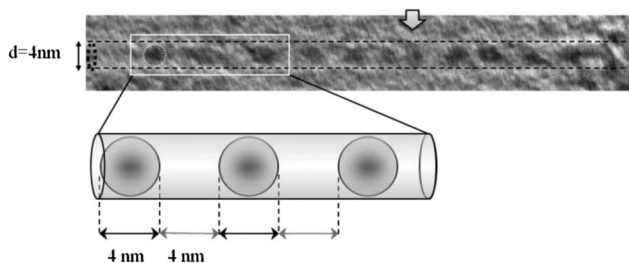


**Fig. 6** Bismuth nanoparticles with diameter  $d = 4$  nm and spacing of 4 nm incorporated in a mesoporous silica matrix ( $d_{\text{pore}} = 4$  nm). Arrow : nanoparticle which disturbs the periodic arrangement.

synthesis tests, it appears to be difficult to reduce this distance while preserving the spherical geometry of the nanoparticles. This shape parameter remains important because the surface roughness of nanoparticles in nanostructured materials influences their thermoelectric properties.<sup>44</sup> In our model, the filtration of the electrons depends at the same time on the distance between nanoparticles, and on the chemical composition of the spaces between them. Various vacuum pumping tests on materials show that it is possible to introduce a gas within the mesopores and control its pressure. This approach should make possible to adjust the thermionic emission and thus to filter the electrons according to their energy.

### (b) Crystallographic study of the Bi incorporated nanoparticles

The crystallinity of the nanoparticles was confirmed using dark field imaging, electron diffraction, and X-ray diffraction. In dark field imaging, all the particles aligned in the channels of the porous structure are not diffracting at the same time. This means they do not lie along the same crystallographic projection. Note also that a strong blinking of the particles was observed during the characterization. The energy of the electron beam induces a quick rotation of the particles. Consequently, the TEM dark-field image shown in Fig. 7 only gives a partial signature of the nanoparticles present in the mean time in the channels (Fig. 7a).

Analyses by electronic diffraction and XRD show that the crystalline phase of the nanoscaled particles is rhombohedral with lattice parameters equal to  $a = 4.5288$  Å and  $c = 11.8620$  Å, same as the bulk crystal (JCPDS 05-0519) (Fig. 7b).

The width of the lines is in agreement with the broadening classically noted for nanomaterials containing bismuth.<sup>45</sup>

In order to study the possible changes in the crystallographic structure of bismuth related to its confinement, we studied the Fourier transforms of HRTEM images of the nanoparticles. The calibration of the images in reciprocal space was carried out from a diffraction pattern of gold. 200 line yielding a lattice spacing  $d = 2.04$  Å was used. This calibration leads to a precision of about 5% on measurements of the  $d_{hkl}$  distances regarding bismuth. Analyses confirm that a great number of particles crystallize in a hexagonal structure. However, for the smallest particles, close to 4 nm in diameter, a centred cubic structure was observed. Less than 5% of the analysed nanoparticles show this feature. Fig. 8 shows an example of a cubic

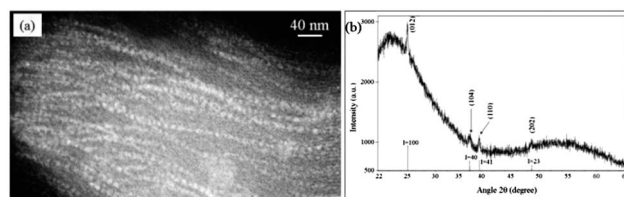


**Fig. 7** (a) TEM dark-field image of bismuth metal nanoparticles developed *in situ* in a mesoporous silica ( $d_{\text{pore}} = 7$  nm). (b) X-ray diffraction pattern obtained with Bragg-Brentano configuration ( $\theta/2\theta$  mode) of silica containing bismuth metal nanoparticles.

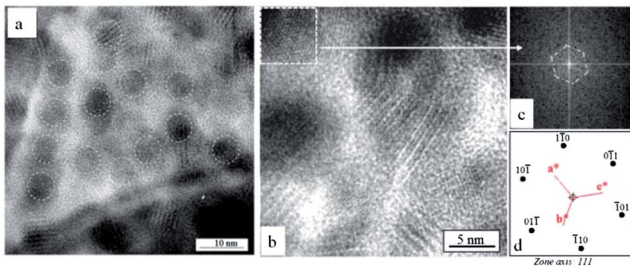


**Fig. 8** High-resolution micrographs of bismuth nanoparticles confined in (a) mesoporous silica; (b) HR image with high magnification; (c) HR Fourier Transform of nanoparticles; (d) diffraction pattern of a centred cubic lattice directed parallel to the zone axis [111] according to CaRine.

bismuth nanoparticle incorporated in the silica matrix. Indeed, the Fourier transform show distances that cannot be explained with the rhombohedral cells. Alternatively, the symmetry observed is consistent with the diffraction pattern of a centred cubic lattice directed according to the zone axis [111] (calculated using CaRine™ crystallography software).

Indexation of the diffraction spots enables us to evaluate the cubic cell parameter, that is equal to  $a = (3.7 \pm 0.2) \text{ \AA}$ . This result shows that confined bismuth nanoparticles crystallize in a cubic structure, a phenomenon that is normally observed at high pressures. This result is consistent with other previously published data. Indeed, Schaufelberger *et al.*<sup>46</sup> have shown that, under a pressure of 90 kPa, bismuth transforms to a cubic structure. It was also reported by E. A. Olson *et al.*<sup>47</sup> that they observed a small reduction in the  $c/a$  lattice parameter ratio for Bi particles below 4 nm in radius.

Taking into account its Fermi surface, this crystalline phase is of interest due to its isotropic properties that make it possible to avoid effects arising from the orientation of the crystal planes of the element and from the resulting differences in the effective mass of electrons.

## Conclusions

A new approach for synthesizing and stabilizing metal bismuth nanoparticles within mesoporous silica based on ionizing irradiation of bismuth salt solutions is presented. Owing to this method, metallic bismuth in the form of particles of nanometric size was incorporated. This synthesis method provides a simple solution allowing obtaining, at the same time, a regular spacing of the nanoparticles and a homogeneous particle size distribution. The adjustments of spacing and diameter of the nanoparticles are obtained by “fine-tuning” the pore diameter of the mesoporous silica, the initial bismuth salt concentration, and the dose rate of the irradiation. Indeed, bismuth nanoparticles with either a mean diameter of 7 nm and a mean spacing of 2 nm, or a mean diameter of 4 nm and a mean spacing of 4 nm, were homogeneously incorporated. When the Bi nanoparticle size is close to 4 nm, a little known cubic structure of this element was identified that is, all the more, interesting because of its potentially isotropic conductivity. Furthermore, nanocomposites containing nanoparticles with a

diameter of 7 nm and a spacing of 2 nm are very interesting as this periodicity could have the advantage of decreasing the conduction of the phonons while at the same time allowing filtration of the electrons by thermionic emission.

This type of nanostructured materials offers the possibility of simultaneously adjusting physical parameters related to quantum confinement, phonon-blocking/electron transmitting and electron filtering barrier properties. The facility of adjustment of these parameters also opens up new avenues for investigating quantum confinement as well as thermoelectric materials.

## Acknowledgements

This work is supported by the ADEME (French Environment and Energy Management Agency). We would like to thank all our many co-workers in this project and, in particular, the Institute for Radioprotection and Nuclear Safety at Saclay (IRSN) for kindly providing access to its gamma irradiation facilities. We also thank F. Warmont for TEM measurements and A. Smock for his illustration.

## Notes and references

- 1 J. P. Heremans, C. M. Thrush, D. T. Morelli and M.-C. Wu, *Phys. Rev. Lett.*, 2002, **88**, 216801.
- 2 W. Xie, J. He, H. J. Kang, X. Tang, S. Zhu, M. Laver, S. Wang, J. R. D. Copley, C. M. Brown, Q. Zhang and T. M. Tritt, *Nano Lett.*, 2010, **10**, 3283–3289.
- 3 P. Pichanusakorn and P. Bandaru, *Mater. Sci. Eng.*, 2010, **67**, 19–63.
- 4 J. M. O. Zide, D. Vashaee, Z. X. Bian, G. Zeng, J. E. Bowers, A. Shakouri and A. C. Gossard, *Phys. Rev. B: Condens. Matter Mater. Phys.*, 2006, **74**, 205335.
- 5 K. Biswas, J. He, Q. Zhang, G. Wang, C. Uher, V. P. Dravid and M. G. Kanatzidis, *Nat. Chem.*, 2011, **3**, 160–166.
- 6 L. D. Hicks and M. S. Dresselhaus, *Phys. Rev. B: Condens. Matter Mater. Phys.*, 1993, **47**, 12727.
- 7 Y.-M. Lin and M. S. Dresselhaus, *Phys. Rev. B: Condens. Matter Mater. Phys.*, 2003, **68**, 075304.
- 8 N. F. Hinsche, B. Yu. Yavorsky, I. Mertig and P. Zahn, *Phys. Rev. B: Condens. Matter Mater. Phys.*, 2011, **84**, 165208.
- 9 R. J. Mehta, Y. Zhang, C. Karthik, B. Singh, R. W. Siegel, T. Borca-Tasciuc and G. Ramanath, *Nat. Mater.*, 2012, **11**, 233–240.
- 10 G. Zhou, L. Li and G. H. Li, *Appl. Phys. Lett.*, 2010, **97**, 023112.
- 11 R. Boldt, M. Kaiser, D. Khler, F. Krumeich and M. Ruck, *Nano Lett.*, 2010, **10**, 208–210.
- 12 Y. Qi, Z. Wang, M. Zhang, F. Yang and X. Wang, *J. Mater. Chem. A*, 2013, Advance Article.
- 13 T. C. Harman, P. J. Taylor, M. P. Walsh and B. E. LaForge, *Science*, 2002, **297**, 2229–2232.
- 14 R. Venkatasubramanian, E. Siivola, T. Colpitts and B. O’Quinn, *Nature*, 2001, **413**, 597–602.
- 15 G. Chen, *Phys. Rev. B: Condens. Matter Mater. Phys.*, 1998, **57**, 14958–14973.
- 16 J. R. Szczech, J. M. Higgins and S. Jin, *J. Mater. Chem.*, 2011, **21**, 4037–4055.
- 17 A. Yokozeki and D. G. Stein, *J. Appl. Phys.*, 1978, **49**, 2224.

- 18 Y.-M. Lin, X. Sun and M. S. Dresselhaus, *Phys. Rev. B: Condens. Matter Mater. Phys.*, 2000, **62**, 4610.
- 19 M. R. Black, P. L. Hagelstein, S. B. Cronin, Y. M. Lin and M. S. Dresselhaus, *Phys. Rev. B: Condens. Matter Mater. Phys.*, 2003, **68**, 235417.
- 20 W. Shim, J. Ham, K. I. Lee, W. Y. Jeung, M. Johnson and W. Lee, *Nano Lett.*, 2009, **9**, 18–22.
- 21 Y. Gao, H. Niu, C. Zeng and Q. Chen, *Chem. Phys. Lett.*, 2003, **367**, 141–144.
- 22 A. Boukai, K. Xu and J. R. Heath, *Adv. Mater.*, 2006, **18**, 864–869.
- 23 E. Condrea and A. Nicorici, *Solid State Commun.*, 2010, **150**, 118–121.
- 24 M. E. Siemens, Q. Li, R. G. Yang, K. A. Nelson, E. H. Anderson, M. M. Murnane and H. C. Kapteyn, *Nat. Mater.*, 2010, **9**, 26–30.
- 25 A. A. Balandin and O. L. Lazarenkova, *Appl. Phys. Lett.*, 2003, **82**, 415–417.
- 26 R. Yang and G. Chen, *Mater. Integr.*, 2005, **18**, 31–36.
- 27 R. Venkatasubramanian, E. Siivola, T. Colpitts and B. O'Quinn, *Nature*, 2001, **413**, 597–602.
- 28 T. C. Harman, P. J. Taylor, D. L. Spears and M. P. Walsh, *J. Electron. Mater.*, 2000, **29**, 1–2.
- 29 S. V. Faleev and F. Léonard, *Phys. Rev. B: Condens. Matter Mater. Phys.*, 2008, **77**, 214304.
- 30 J. Zhou and R. Yang, *Phys. Rev. B: Condens. Matter Mater. Phys.*, 2010, **82**, 075324.
- 31 A. Yadav, K. P. Pipe, W. Ye<sup>2</sup> and R. S. Goldman, *J. Appl. Phys.*, 2009, **105**, 093711.
- 32 D. Vashaee and A. Shakouri, *Phys. Rev. Lett.*, 2004, **92**, 106103.
- 33 J. M. O. Zide, J.-H. Bahk, R. Singh, M. Zebarjadi, G. Zeng<sup>2</sup>, H. Lu, J. P. Feser, D. Xu, S. L. Singer, Z. X. Bian, A. Majumdar, J. E. Bowers, A. Shakouri and A. C. Gossard, *J. Appl. Phys.*, 2010, **108**, 123702.
- 34 J. M. O. Zide, D. Vashaee, Z. X. Bian, G. Zeng, J. E. Bowers, A. Shakouri and A. C. Gossard, *Phys. Rev. B: Condens. Matter Mater. Phys.*, 2006, **74**, 205335.
- 35 D. Vashaee and A. Shakouri, *J. Appl. Phys.*, 2007, **101**, 053719.
- 36 D. M.-T. Kuo and Y.-C. Chang, *Phys. Rev. B: Condens. Matter Mater. Phys.*, 2010, **81**, 205321.
- 37 T. Coquil, E. K. Richman, N. J. Hutchinson, S. H. Tolbert and L. Pilon, *J. Appl. Phys.*, 2009, **106**, 034910.
- 38 F. Y. Yang, K. Liu, K. Hong, D. H. Reich, P. C. Searson and C. L. Chien, *Science*, 1999, **284**, 1335.
- 39 D. Zhao, Q. Huo, J. Feng, B. F. Chmelka and G. D. Stucky, *J. Am. Chem. Soc.*, 1998, **120**, 6024–6036.
- 40 S. Willemin, G. Arrachart, L. Lecren, J. Larionova, T. Coradin, R. Clerac, T. Mallah, C. Guerin and M. Sanchez, Immobilisation of single molecule magnets in mesoporous silica hosts, *New J. Chem.*, 2003, **27**, 1533–1539.
- 41 R. Benoit, M. L. Saboungi, M. Tréguer-Delapierre, B. H. Milosavljevic and D. Meisel, *J. Phys. Chem. A*, 2007, **42**, 10640.
- 42 C. Vossloh, M. Holdenried and H. Micklitz, *Phys. Rev. B: Condens. Matter Mater. Phys.*, 1998, **58**, 12422–12426.
- 43 A. Wurl, M. Hyslop, S. A. Brown, B. D. Hall and R. Monot, *Eur. Phys. J. D*, 2001, **16**, 205–208.
- 44 S. Wang and N. Mingo, *Phys. Rev. B: Condens. Matter Mater. Phys.*, 2009, **79**, 115316.
- 45 H. Yu, P. C. Gibbons and W. E. Buhro, *J. Mater. Chem.*, 2004, **14**, 595–602.
- 46 Ph. Schaufelberger, H. Merx and M. Contre, *High Temperatures – High Pressures*, 1973, **5**, 221–230.
- 47 E. A. Olson, M. Yu. Efremov, M. Zhang, Z. Zhang and L. H. Allen, *J. Appl. Phys.*, 2005, **97**, 034304.